Equilibrium phase diagrams for dislocation free self-assembled quantum dots

István Daruka and Albert-László Barabási

Citation: Applied Physics Letters **72**, 2102 (1998); doi: 10.1063/1.121289
View online: http://dx.doi.org/10.1063/1.121289
View Table of Contents: http://scitation.aip.org/content/aip/journal/apl/72/17?ver=pdfcov
Published by the AIP Publishing

Equilibrium phase diagrams for dislocation free self-assembled quantum dots

István Daruka and Albert-László Barabási[a)]
Department of Physics, University of Notre Dame, Notre Dame, Indiana 46556

(Received 26 November 1997; accepted for publication 24 February 1998)

The equilibrium theory of self-assembled quantum dot (SAQD) formation can account for many of the experimentally observed growth modes. Here, we show that despite the large number of material constants entering the free energy of strained islands, there are only four topologically different phase diagrams describing the SAQD formation process. We derive each of these phase diagrams and discuss the physical properties of the predicted growth modes. © *1998 American Institute of Physics.* [S0003-6951(98)00317-9]

Heteroepitaxial growth of highly strained structures has gained interest lately as it offers the possibility to fabricate nanoscale islands with very narrow size distribution.[1] Such islands have been coined self-assembling quantum dots (SAQD). Although the understanding of the basic mechanisms determining the size and the distribution of the islands is hampered by the coexistence of equilibrium and nonequilibrium effects,[1,2] equilibrium studies have been quite successful in capturing the key features of SAQD formation.[3–6] The starting point of the equilibrium calculations is the derivation of the free energy that incorporates the effect of strain and island formation. Along these lines Shchukin *et al.*[4] predicted that for a certain range of material constants stable islands can exist on the surface. We have recently shown that by incorporating the contribution of the wetting layer in the free energy, the resulting equilibrium phase diagram can account for most of the experimentally observed growth modes and island configurations.[3] This phase diagram also provides a detailed description of the main equilibrium phases, such as the Frank van der Merve (FM), Stranski-Krastanow (SK), and Volmer-Weber (VW) growth modes. However, a major shortcoming of the equilibrium calculations lies in the large number of unknown material constants that enter the free energy. Many of these parameters are phenomenological and often even their order of magnitude is unknown. Since the number of the unknown parameters is rather high (as many as nine independent parameters are cited in Ref. 4), we can question the generality of the phase diagram derived for a particular choice of these parameters. These unknown parameters might lead to a large number of topologically distinct phase diagrams, limiting the predictive power of the equilibrium theory.

In this letter we show that, despite the large number of material constants, there are only four topologically distinct phase diagrams describing the equilibrium properties of SAQD. This implies that, independent of the materials involved in the growth process, the phase diagram describing the growth modes is topologically equivalent to one of the diagrams described here. We find that the difference between the phase diagrams is encoded in the relative strength of the surface energy and that one can continuously go from one phase diagram to the other in a well defined order by increasing the surface energy.

Model and free energy— We assume that H monolayers of atom A with lattice constant d_A are deposited on top of the substrate B with lattice constant d_B, and the system is allowed to equilibrate. Due to the lattice mismatch, $\epsilon=(d_A-d_B)/d_B$, in equilibrium one expects that a certain fraction of atom A forms a wetting film of n_1 monolayers, and the rest of the material ($H-n_1$ monolayers) is distributed in three-dimensional (3D) islands.

The relevant thermodynamic potential density is the free energy per atom, $f=u-Ts$, where u is the internal energy density, T is the temperature and s is the entropy density of the system. However, one can show that at moderate growth temperatures the entropic contribution to f is negligible,[7] thus $f\approx u$, where

$$u(H,n_1,n_2,\epsilon)=E_{\mathrm{ml}}(n_1)+n_2E_{\mathrm{isl}}+(H-n_1-n_2)E_{\mathrm{rip}}. \tag{1}$$

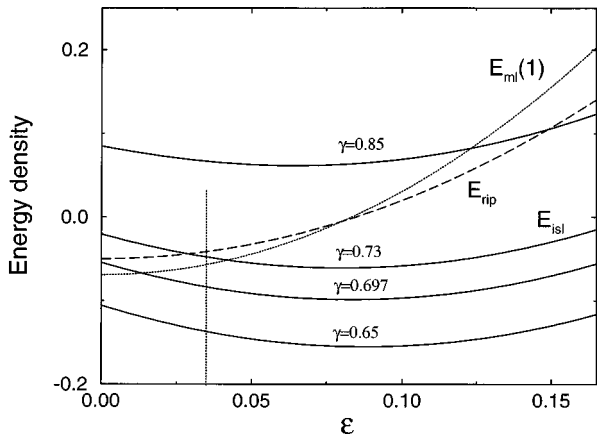

FIG. 1. Energy densities (energy per atom) shown as a function of the lattice misfit ϵ. The curves correspond to the wetting film energy (dotted line), ripened island energy (dashed line), and the finite island energy (solid lines). The energy of the finite islands is plotted for four different surface energies: $\gamma=0.85$, 0.73, 0.697, and 0.65, each defining a topologically distinct phase diagram (see Fig. 2). The parameters used to obtain these curves are $a=1$, $C=10E_0$, $\Phi_{\mathrm{AA}}=0.1E_0$, $\Phi_{\mathrm{AB}}=0.1192E_0$, $g=0.7$, $p=1.73$, and $b=10$.

a)Electronic mail: alb@nd.edu

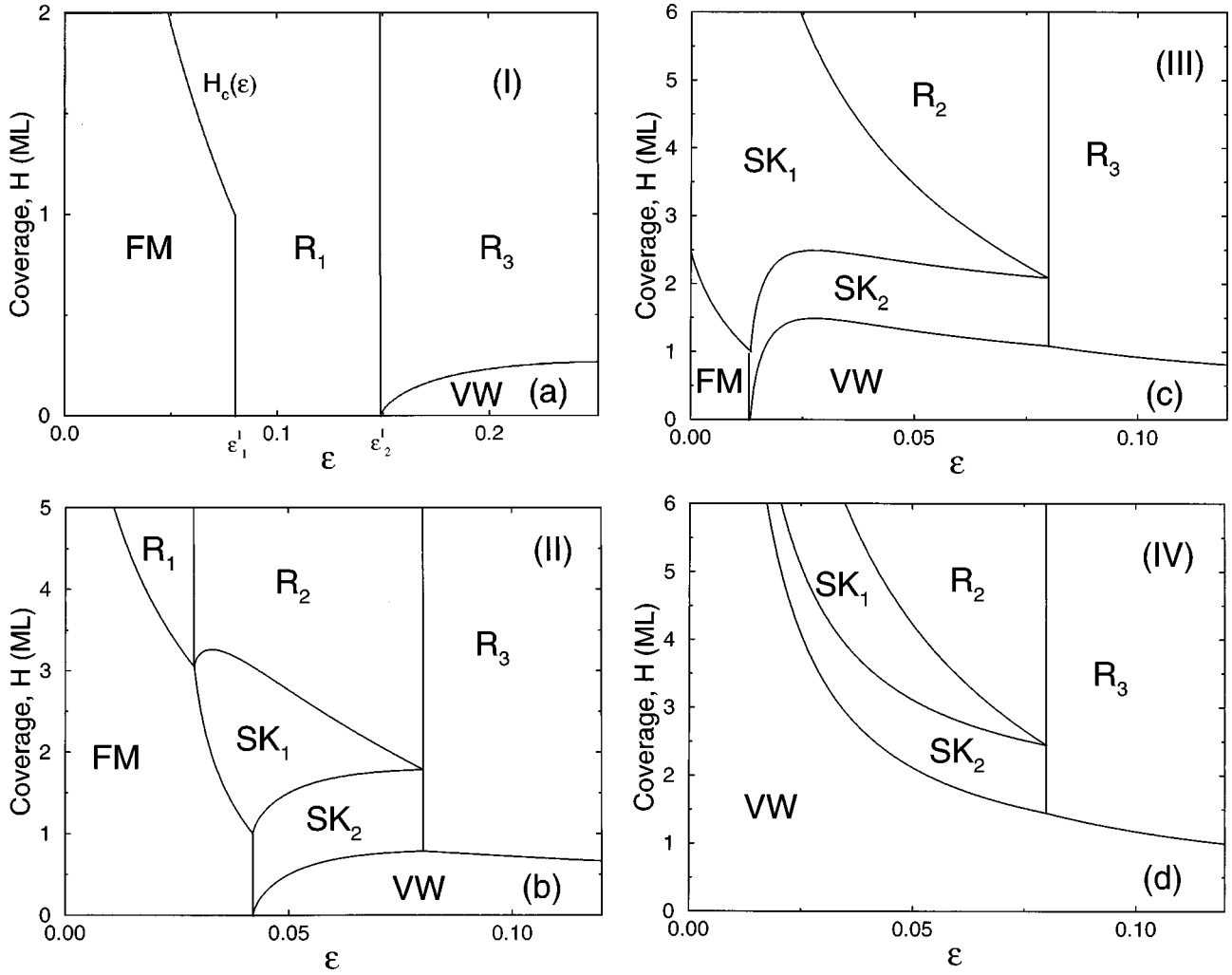

FIG. 2. Equilibrium phase diagrams for four different surface energies (γ) as a function of the coverage H and misfit ϵ. The corresponding surface energies are (a) γ=0.85, (b) 0.73, (c) 0.697, and (d) 0.65, corresponding to (a)–(d), respectively. The rest of the parameters are the same as in Fig. 1.

The first term provides the contributions of the n_1 strained overlayers. This term is an integral over the binding and the elastic energy densities[3]

$$E_{\mathrm{ml}}(n_1)=\int_0^{n_1} dn\{G+\Delta[(\Theta(1-n)+\Theta(n-1)e^{-(n-1)/a}]\}, \tag{2}$$

where $G=C\epsilon^2-\Phi_{\mathrm{AA}}$, $\Delta=\Phi_{\mathrm{AA}}-\Phi_{\mathrm{AB}}<0$, C is a Young modulus dependent material constant, $-\Phi_{\mathrm{AA}}$ ($-\Phi_{\mathrm{AB}}$) is the energy of an AA (AB) bond, and $\Theta(x)=0$ if $x<0$ and $\Theta(x)=1$ if $x>0$. The constant $a>0$ describes the decay of the short-range intermolecular forces between the substrate and the wetting film.

We distinguish between the stable, finite size 3D islands and the ripened ones, which grow indefinitely. These two types of islands give rise to the second and third terms in Eq. (1). The second term in Eq. (1) describes the free energy per atom of pyramidal islands and the island-island interaction[3]

$$E_{\mathrm{isl}}=gC\epsilon^2-\Phi_{\mathrm{AA}} +E_0\left(-\frac{2}{x^2}\ln e^{1/2}x+\frac{\gamma-p\epsilon}{x}+\frac{\beta(n_2)}{x^{3/2}}\right), \tag{3}$$

where $x=L/L_0$ is the reduced island size, L_0 is a material dependent characteristic length and g is a form factor ($0<g<1$).[4] The second term stands for the binding energy. The first term in the parenthesis accounts for the surface stresses (stress discontinuities at the island edges),[4] while the second term is the sum of the surface stress cross term (with coefficient $-p$) and the surface energy term (with coefficient γ), the latter depending on the facet orientation.[3,4] The last term describes the island-island repulsive interaction with the coupling $\beta(n_2)=b\epsilon^2 {n_2}^{3/2}$, where b is a material constant and n_2 is the number of monolayers distributed in finite islands. In the following, we refer to $[-2/x^2\ln e^{1/2}x-p\epsilon/x+\beta(n_2)/x^{3/2}]$ in Eq. (3) as elastic energy.

The total energy density of the ripened islands can be obtained from Eq. (3) by taking the limit $x\to\infty$, providing $E_{\mathrm{rip}}=gC\epsilon^2-\Phi_{\mathrm{AA}}$, which is multiplied by the total number of atoms stored in the ripened islands, $(H-n_1-n_2)$.

Classification of the Phase Diagrams— For a particular coverage H and lattice misfit ϵ, the surface morphology is determined by the value of the monolayer energy $E_{\mathrm{ml}}(H,\epsilon)$, the island energy per atom, $E_{\mathrm{isl}}(H,\epsilon)$, and the ripened island energy density $E_{\mathrm{rip}}(\epsilon)$. The energy densities $E_{\mathrm{ml}}(H,\epsilon)$ and $E_{\mathrm{isl}}(H,\epsilon)$ increase monotonically with H. As we start depositing material on the surface, the structure with the lowest energy forms first. The order of the phases for a particular phase diagram is encoded in the order in which these energy

density functions intersect each other (Fig. 1). It can be seen in Fig. 1 that $E_{\rm isl}$ can intersect $E_{\rm ml}(1)$ and $E_{\rm rip}$ in only four different ways, which lead to *four topologically different phase diagrams*.

As an illustration, consider $\epsilon=0.035$ (dotted vertical line in Fig. 1) and $\gamma=0.73$, the corresponding phase diagram shown in Fig. 2(b). For this misfit, $E_{\rm ml}(1)$ has the lowest energy, thus the first deposited monolayer forms a uniform wetting film corresponding to the FM phase. The deposition of more material increases the thickness of the wetting film and the strain energy stored in the uniformly compressed wetting film. When the total energy reaches $E_{\rm isl}$, the newly deposited material will be partitioned between the wetting film and the finite islands formed on top of the wetting film. This defines the first critical thickness and a transition to the SK_1 growth mode, marked by the coexistence of stable islands (SAQD) and a wetting film. Depositing even more material, both the wetting film and the islands develop further, their energy densities increase until they reach the formation energy of ripened islands, $E_{\rm rip}$. After this second critical thickness, that marks the onset of ripening, all the deposited material will contribute to the ripened islands, thus the wetting film and the finite islands will not grow further in R. From Fig. 1 we can also determine the critical misfits for a particular phase diagram. There are two critical misfits for $\gamma=0.73$: at $\epsilon=0.029$, where the finite island energy intersects the ripening energy, and at $\epsilon=0.042$, where the finite island energy intersects the wetting film energy.

The four phase diagrams in Figs. 2(a)–2(d), which display the growth modes as a function of the lattice misfit ϵ and the coverage H, correspond to four different γ values. Next we briefly discuss each of these phase diagrams.

Phase Diagram I [PDI, Fig. 2(a)]: This phase diagram corresponds to the highest value of γ, and a typical case can be followed using $\gamma=0.85$ (see Fig. 1). For small lattice misfits ($\epsilon<\epsilon_1^I$) and for $H<H_c(\epsilon)$ we have wetting film formation, corresponding to the FM growth mode. Islands in general lead to the relaxation of the strain energy, but have a larger surface energy due to the larger surface area compared to that of the flat wetting film. Since γ is large, in this regime the cost of creating islands with larger surface area (surface energy), is larger than the energy release provided by the strain relaxation, and islands cannot form. For intermediate misfits ($\epsilon_1^I<\epsilon<\epsilon_2^I$) the elastic relaxation is smaller than the surface energy, but large enough to win over the wetting film energy, leading to ripening at $H=0$. Since the relaxation energy depends on ϵ^2, for large misfits ($\epsilon>\epsilon_2^I$) the elastic relaxation terms overcome the surface energy, resulting in the formation of finite islands (VW growth) for small coverages. However, for larger coverages ($H>H_c$) the increased island–island interaction leads to ripening (R_3). Note that while in R_1 only ripened islands are present, R_3 consists of coexisting finite and ripened islands.

Phase Diagram II [PDII, Fig. 2(b)]: This phase diagram has the same topology and growth modes as the one discussed in detail in Ref. 3, thus we will not discuss it further here.

Phase Diagram III [PDIII, Fig. 2(c)]: The structure of this phase diagram is similar to that of PDII. The only difference is that the FM-R_1 phase boundary line is missing, implying that for *any misfit there is a coverage at which stable finite islands are present.*

Phase Diagram IV [PDIV, Fig. 2(d)]: The last phase diagram corresponds to the lowest value of the surface energy. The structure of this diagram is even simpler, marked by the disappearance of the FM phase. All the other phases are the same as for PDIII.

In conclusion we have shown that, despite the large number of parameters of the free energy describing SAQD, there are only four topologically distinct equilibrium phase diagrams. By increasing the surface energy parameter, γ, one can continuously go through the succession of the four phase diagrams, allowing us to interpret the topological differences in terms of γ. Furthermore, the topology of these phase diagrams allows us to draw some general conclusions regarding the equilibrium properties of SAQD. As a general rule, we find that independent of the material constants, for large coverages the system reaches a ripening phase. Thus, to grow islands that are stable under annealing one needs to control carefully the amount of the deposited material. The calculation predicts four major growth modes (FM, SK, VW, and R) each of which have been observed experimentally.[1] The island size, island density, and the distribution of the material between the islands and the wetting film can also be calculated for each of these transitions and growth modes.[3]

[1] For a recent review, see W. Seifert, N. Carlsson, M. Miller, M.-E. Pistol, L. Samuelson, and L. R. Wallenberg, J. Progr. Crystal Growth Charact. Mater. **33**, 423 (1996); P. M. Petroff and G. Medeiros-Ribeiro, MRS Bull. **21**, 50 (1996).

[2] H. T. Dobbs, D. D. Vvedensky, A. Zangwill, J. Johansson, N. Carlsson, W. Seifert, Phys. Rev. Lett. **79**, 897 (1997); A.-L. Barabási, Appl. Phys. Lett. **70**, 2565 (1997); B. G. Orr, D. Kessler, C. W. Snyder, and L. Sander, Europhys. Lett. **19**, 33 (1992); A. Madhukar, J. Cryst. Growth **163**, 149 (1996).

[3] I. Daruka and A.-L. Barabási, Phys. Rev. Lett. **79**, 3708 (1997).

[4] V. A. Shchukin, N. N. Ledentsov, P. S. Kop'ev, and D. Bimberg, Phys. Rev. Lett. **75**, 2968 (1995).

[5] J. Tersoff, Phys. Rev. B **43**, 9377 (1991); C. Roland and G. H. Gilmer, *ibid.* **47**, 16286 (1993).

[6] T. I. Kamins, E. C. Carr, R. S. Williams, and S. J. Rosner, J. Appl. Phys. **81**, 211 (1997); G. Medeiros-Ribeiro, A. M. Bratkovski, T. I. Kamins, D. A. A. Ohlberg, and R. S. Williams, Science **279**, 353 (1998); M. Krishnamurthy, B.-K. Yang, and J. D. Weil, Appl. Phys. Lett. **70**, 49 (1997).

[7] At high growth temperatures, entropy increases the adatom concentration and can modify the exact position of the phase boundaries. However, we expect that in the experimentally relevant temperature range the *topology* of the phase diagram will not be affected by the entropy. Note that, following different arguments, similar conclusions have been reached by S. R. Williams (private communication).